Imaging of Cancer Cells using Gold Nanoparticels and Fluorescent Dyes by Multiphoton Microscopy

Xiaochao Qu
The Key Laboratory of Biomedical Information Engineering of Ministry of Education, School of Life Science and Technology, Xi'an Jiaotong University, No.28, Xianning West Road, Xi'an 710049, China.
E-mail: xiaochaoqu@gmail.com

Jing Wang
Zhenxi Zhang
The Key Laboratory of Biomedical Information Engineering of Ministry of Education, School of Life Science and Technology, Xi'an Jiaotong University, No.28, Xianning West Road, Xi'an 710049, China.

Ramtin Rahmanzadeh
Koop Norbert
Gereon Hüttmann
University Lübeck, Institute of Biomedical Optics, Peter-Monnik-Weg 4, D-23562 Lübeck, Germany
E-mail: huettmann@bmo.uniluebeck.de

ABSTRACT

Due to the special optical properties, optical probes including metal nanoparticles (NPs), quantum dots, and fluorescent dyes, are increasingly used as labeling tools in biological imaging. Using multiphoton microscopy and fluorescence lifetime imaging (FLIM) system, we recorded the images from gold NPs conjugated to monoclonal ACT1 antibody, fluorescence dye Alexa 488 (A488) conjugated to ACT1, and dye Hoechst 33258 (H258) after incubation in cell culture with lymphoma cell lines (Karpas 299). From these images, we can easily discriminate the imaging difference due to the different emission intensity, distinct fluorescence lifetime between cells and the three optical probes. Our results present that Au-ACT1 conjugates and A488-ACT1 conjugates bind homogeneously and specifically to the surface of cells, and H258 is stained on cell nuclear. Compared with Karpas 299 cells, stronger emission intensity of gold NPs is observed at the same excitation power; and it can be comparable to, even more than that of fluorescent dyes in the same laser excitation. Gold NPs has more photostable than the other fluorescent probes. These results suggest gold NPs are useful for the study of cellular imaging and cancer diagnosis as molecular labeling tools.

Keywords: Multiphoton microscopy, fluorescence lifetime imaging, gold nanoparticles, Alexa 488, Hoechst 33258, Karpas 299 cells

Address all correspondence to Gereon Hüttmann, Institute of Biomedical Optics, University Lübeck, Peter-Monnik-Weg 4, D-23562 Lübeck, Germany. Tel: ++49–451–500–6530. Fax: ++49–451–5646. E-mail: huettmann@bmo.uniluebeck.de

1. INTRODUCTION

Nowadays, basic biomedical research centers on the investigation of dynamic processes in normal or disease tissues. Optical techniques for cellular imaging are opening new avenues into exploration of microscopic structure and dynamics for diagnostic application and biological imaging. And the imaging effects will be enhanced when using optical probes as biomarkers[1, 2]. Currently used optical probes include fluorescent dyes, noble metal nanoparticles, etc. Conventional fluorescent dyes have small Stokes shifts, which resulting in reduced detection sensitivity. And they undergo permanent photobleaching, compromising the ability to view the same region repeatedly or over time. Quantum Dots have recently been utilized as fluorescent probes for labeling experiments[3, 4]. They can resist photobleaching for a long time, but potential cytotoxicity is the major problem for their application in vitro and in vivo. Metal noble NPs, in particular gold, have received widespread interest in their use due to their easy preparation with controlled diameters, ready conjugation with biomolecules, and highly controlled optical properties[5]. Since these nanoparticles do not suffer from photobleaching and phototoxicity[6], they are considered as attractive alternatives for specific biological labeling[7, 8].

Many previous studies have presented that optical microscopic techniques, such as confocal scanning microscopy, multiphoton microscopy, and optical coherence microscopy were developed to study cells or tissue, which is labeled or unlabeled by fluorescent dyes, or gold NPs[9, 10]. Here we consider, in a different approach, detection of optical probes by means of nonlinear optical methods. Multiphoton microscopy has gained significant popularity in biomedical imaging in recent years. Using ultrafast near-infrared laser system, the nonlinear excitation has provided important advantages in its ability to acquire images[11]. Since the multiphoton signal is generated only at the vicinity of the focal spot, where the photon flux is high, the imaging process has enhanced axial depth discrimination and reduced sample photodamage.

In the present work, we used a multiphoton microscope and fluorescence lifetime imaging (FLIM) system to image lymphoma cell lines Karpas 299, which was incubated with ACT1 antibody conjugated gold NPs, ACT1 conjugated A488, and H258. The optical properties of these optical probes incubated in living cells were compared for different experiment conditions. Our basic study demonstrates that gold NPs, A488, and H258 with high efficient emission, can strengthen cellular imaging. The analysis for decay curve of the fluorescent signal with a particular interesting region by TCSPC has distinguished the different lifetime between optical probes and cells. It is found that the multiphoton FLIM based on gold NPs can offer potential techniques for biological labeling and imaging.

2. MATERIALS AND METHODS

2.1 Multiphoton Imaging System

The multiphoton imaging system DermaInspect (JenLab, Jena, Germany) is designed for deep-tissue optical tomography. A titanium-sapphire laser (MaiTai/Spectra Physics/Darmstadt, 80MHz, 75 fs) was used as an excitation source with a tuning range of 710 to 920nm, a mean output power of 900mw at 800nm. The scanning module contains a motorized shutter, beam attenuator, and a two axis galvoscanner. Other components include a 40× oil-immersion lens (Zeiss, Goettingen, Germany, numerical aperture (NA) =1.30, working distance =140 mm), and a beam splitter and a short-pass filter (BG39, Schott, Mainz, Germany) that enabled the excitation light to reflect onto the sample and wavelengths between 350 and 600 nm to transmit to the detector. Then the signal was detected by a

photon-counting photomultiplier tube module (PMT, H7732-01, Hamamatsu, Herrsching, Germany).

2.2 Fluorescence Lifetime Imaging Mode

Fluorescence lifetime imaging, which was achieved here by time-correlated single-photon counting (TCSPC) is a useful contrast enhancing method that provides information related to the microenvironment with spatial resolution. Intensity and signal from the excited spot of the sample were collected pixel by pixel by a laser scanning unit and a fast photon- counting PMT (PMH-100-0, Becker & Hickl, Berlin, Germany, transient time spread =180 ps) connected to the TCSPC system (SPC-830, Becker & Hickl, Berlin, Germany)[12]. The SPCImage software (Becker & Hickl) was used to analyze the fluorescence lifetime decay curves.

The fluorescence lifetime τ is defined as the average time that the fluorophore is in an excited state prior to returning to its ground state. The measured lifetime decay curve was binned over the pixel of interest and the eight-nearest neighbor pixels. Each set of binned pixels was fit independently. The lifetime decay curve of the pixel of interest was then fit to a exponential decay model:

$$F(t) = \alpha_1 \mathrm{e}^{-t/\tau_1} + \alpha_2 \mathrm{e}^{-t/\tau_2} + \alpha_3 \mathrm{e}^{-t/\tau_3} \qquad (1)$$

where $F(t)$ is the fluorescence intensity at time t after the excitation light has ceased, τ is the fluorescence lifetime and α is the relative contribution of the lifetime component (i.e. $\alpha_1 + \alpha_2 + \alpha_3 = 100\%$). For single exponential model, the amplitude coefficients α_2 and α_3 are set to zero. However, in cases where the fluorescence was measured with a good signal-to-noise ratio (SNR), we will have to switch to a double exponential decay or even go up to three exponential components. These values are used to address a memory in which the detection events are accumulated. To analyze the fluorescence lifetime of specific cellular compartments, region of interest was defined. Curve fitting of a single exponential decay curve was used to calculate a mean fluorescence lifetime for each pixel, which was displayed in color coded images. Multi-exponential decay profiles can therefore be resolved into their lifetime components and relative intensity coefficients[13].The lifetime for the pixel of interest was calculated by finding the global minimum of the χ^2 value. If the model is appropriate, the reduced χ^2 should be displayed. A χ^2 value close to 1 indicates a good fit.

2.3 Cell Lines and Cell Culture

The human lymphoma cell lines Karpas 299 were kindly provided from Forschungszentrum Borstel Leibniz-Zentrum für Medizin und Biowissenschaften, Germany. Cells were routinely grown in suspension culture in a RPMI (Roswell Park Memorial Institute) 1640 (1×) with Hepes and L-Glutamine medium supplemented with 10% fetal calf serum, antibiotic/antimycotic solution (all cell culture media PAA Laboratories, Pasching, Austria) in a 37°C humidified incubator (5% CO2, 95% air).

2.4 Preparing Experimental Samples

1. Au-ACT1 conjugates: Immunogold NPs, which were made of gold NPs with diameters of 30 nm (British Biocell International) and ACT1 antibodies, were prepared according to the method described by Sololov[14]. When Cells were in log phase growth, cell suspension was centrifuged at 1400 rpm for 5 min at 20°C, and then resuspended in phosphate-buffered saline (PBS, pH 7.2, containing 1% bovine serum albumin) with cell densities $\times 10^6$/ml. Then added the Au-ACT1 conjugates to the cell suspension at certain ratios of gold NPs to number of cells, and the compound was incubated for 20 min at 37 °C.

After incubation, they were centrifuged and washed twice, then resuspended in PBS.

2. A488-ACT1 conjugates: A488 (Molecular probes) conjugated with ACT1 antibodies were prepared by the method of immunohistochemistry. Cell staining of A488-ACT1 conjugates was performed as follows. When cell suspension was centrifuged and resuspended in PBS, the conjugates solution was added into the cell suspension at a certain ratio and incubated according to the method as described above. Then the mixture was washed with PBS buffer for two times.

3. Hoechst 33258 is a fluorescent nucleic acid stain for labeling DNA. H258 with 1mg/ml concentration was diluted for 1μg/ml with PBS. After cell suspension was centrifuged and resuspended in PBS, the diluted H258 solution was added into the cell suspension and the mixture was incubated for 1 h in incubator at 37°C. Then the staining solution was rinsed away and replaced by PBS buffer.

After finishing the incubation of cells with fluorescence dye or immunooptical probes, we prepared the experimental samples. On the surface of slides were treated with special material to form a circle. When the prepared compound was fixed on the slide, the sample was used for multiphoton imaging immediately.

3. RESULTS

3.1 Imaging of Karpas 299 Labeled with Au-ACT1 Conjugates

The special linear and nonlinear optical properties of gold NPs are the subject of recent studies[14]. Multiphoton absorption induced luminescence (MAIL) has even been shown to produce efficient luminescence of gold NPs[15]. For this experiment, we used gold NPs of two different diameters (15nm, 30nm) with the same concentration for multiphoton imaging, and compared their luminescence efficiency. Figure 1 shows the intensity images and false-color fluorescence lifetime images of gold NPs with 15nm (a) and 30nm (b). The broad range of emission intensities is observed for gold NPs of the same average diameter from Figure 1(c). Although it is difficult to quantify their differences precisely due to the range of efficiency present for gold NPs of the same average size, we still observed that gold NPs with 30nm exhibited much stronger luminescence than 15nm gold. After experimental determination of the luminescence efficiency for gold NPs with different diameters, 30nm gold is chosen for the following experiments. The other reason of choosing 30nm is that the bigger size is much easier to couple with antibodies according to our experimental experience.

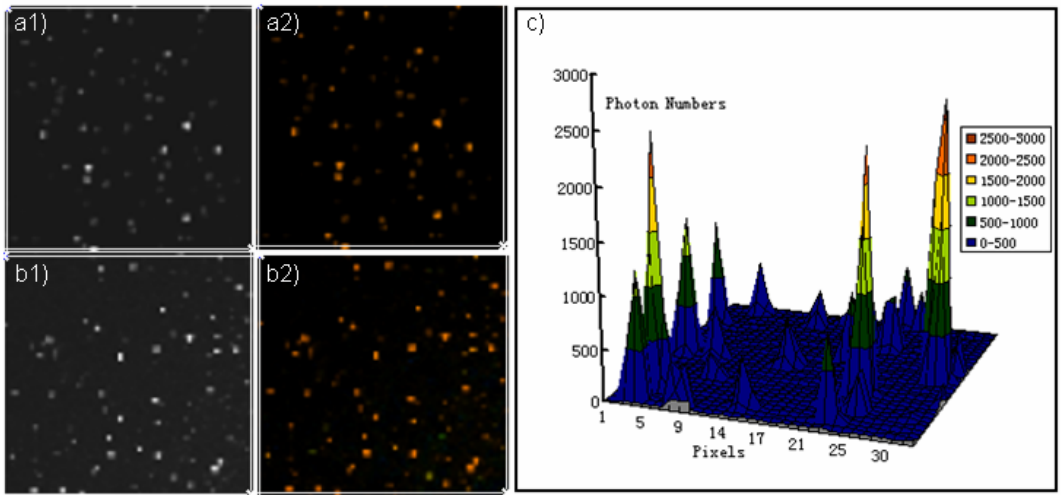

Fig.1. Intensity images and corresponding false-color FLIM images for gold NPs with different diameters: (a) 15nm, (b) 30nm. The size of images is about 20μm (64×64 pixels) (Excitation: 750nm, 20mw; Zoom: 400). A

central region (32×32 pixels) of image in (a) was represented as contour intensity plot, which is shown in (c).

Figure 2 shows intensity images and FLIM images of Karpas 299 cells, and cells incubated with Au-ACT1 conjugates. According to the different lifetimes of cells and gold NPs, there are some distinct differences in images between cells incubated without and with gold NPs.

Multiphoton excited fluorescent microscopy of living cells demonstrated individual cellular component at subcellular resolution. Intensity image of the autofluorescent signal delineated cytoplasm structure such as cellular nucleus (Figure 2(a1)). The corresponding time resolved fluorescence lifetime measurements demonstrated different lifetimes of cell (Figure 2(a2)). The histogram of fluorescence lifetime of Karpas 299 at 750 nm, 20mw laser excitation measured from the decay curves are mean 1800ps for cytoplasmic areas and about 1200 ps for the cellular nucleus.

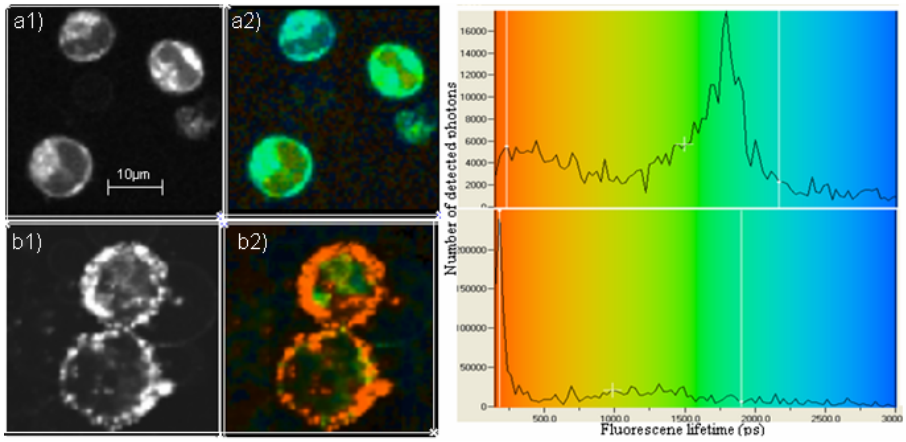

Fig.2. Intensity images, corresponding false-color FLIM images of Karpas 299 cells (a) and cells incubated with Au-ACT1 conjugates (b) (Excitation: 750nm, 20mw; Zoom: 600). Histograms of lifetime distribution of the images in (a) and (b).

ACT1 is a specific antibody to the cell membrane receptors of interleukin-2 (CD25) of Karpas 299. Due to the binding of CD25 with ACT1 on the gold surface, gold NPs are uniformly distributed on the surface of cell membrane of Karpas 299 (Figure 2(b)). Differ from the image in (a), some pixels in Figure 2b are conjugation areas of gold NPs and cell membrane. Due to two lifetimes contained in these areas at least, there needs two or more components to fit in these particular areas, and get an acceptable $\chi 2$ value. For a selected region, the fit curve yields a mean fluorescence lifetime of 355.72ps, two components with a contribution of 90% of 194.9ps and 10% of 1803.6ps component. As depicted in the histogram, the fluorescence lifetime of gold NPs is distributed in the red area, whereas the fluorescence lifetime of cell is typical on the order of 1.0-2.0ns. In our system, the time-resolution is limited by the transit time spread of detector that is about 180 ps for our fast photomultiplier tube.

3.2 Comparison of cells labeled with Au-ACT1 and A488-ACT1 conjugates

The optical properties of fluorescent probe A488 is studied through conjugating it to ACT1 antibody and incubating in Karpas 299 cells as conjugates. As a relatively new molecular probe, dye A488 is brighter and more resistant to photobleaching than conventional fluorescent dyes[16].

As expected, the intensity image and false-color FLIM image showed a distinct staining pattern throughout the surface of cells (Figure 3(a)). Corresponding histogram of lifetime distribution of photons of the image is shown in right column. The blue color comes from fluorescent dye A488, and the mean lifetime is about 3.45 ns. In order to compare the relevant optical properties of gold NPs and

fluorescence dye, another contrast experiment was carried out. The cell suspension was mixed with Au-ACT1 conjugates and A488-ACT1 conjugates respectively and incubated for 20 min. Then washed them for two times with PBS. Prior to the multiphoton imaging experiment, the two mixtures were mixed together uniformly, and prepared as a sample for experiment.

Figure 3(b) shows the intensity image and corresponding discrete false-color FLIM image. According to the different fluorescence lifetime, gold NPs and A488 can be distinguished easily. In the same condition with laser excitation, the emission intensity of gold NPs is much stronger than that of A488. Due to the permanent photobleaching on a time scale, the fluorescence signal of A488 became very week with laser excitation for many minutes. But the emission intensity of gold NPs is photostale steady during this period

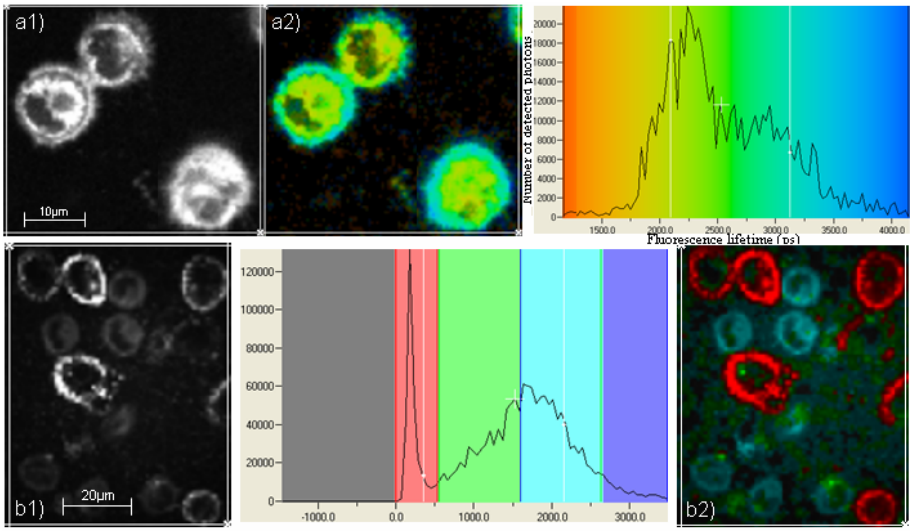

Fig.3. Intensity image (a1), false-color FLIM image (a2) of Karpas 299 cells incubated with A488-ACT1 conjugates (Excitation: 750nm, 25mw; Zoom: 700). Corresponding histogram of lifetime distribution of the image in (a). (b). Intensity image and discrete false-color FLIM image of cells incubated with A488- ACT1 and Au-ACT1 conjugates. And corresponding histogram of lifetime distribution in middle column.

3.3 Imaging of cells labeled with Gold NPs and dyes H258

In this section, we combined gold NPs with fluorescent molecular probes H258 to characterize their individual optical properties using fluorescence lifetime imaging microscopy. H258 is an important staining molecule for cellular DNA in the study of cell and molecular biology. Prior to the imaging experiment, Karpas 299 cell suspension was mixed with Au-ACT1 conjugates and incubated for 20 min, and then H258 solution was added into the mixture for 1h.

Figure 4 displays the images obtained from the cells stained with gold NPs and H258 at 750nm, 15mw laser excitation. The overall acquisition time was 60 seconds. (a) shows the intensity image and FLIM image of sample. Correspongding histogram of lifetime distribution of the image is shown in Figure 4(b). Deconvolution analysis delivers the fluorescence lifetime τ in individual pixels of the image. When fluorescence lifetime was analyzed for specific areas of interest, a significantly longer lifetime of signal was found in nuclear area that was stained by H258 (d), and the shorter one was found in membrane area labeled by gold NPs (c). The blue color comes from H258. Accordingly, we used FLIM to determine the spatial distribution of lifetimes in cells. For the all H258-stained regions, the lifetime was typically flat and devoid of spatial differences. The mean lifetime of H258 is about 2.45 ns, which is comparable to that found in spectroscopic time- resolved measurements[17].

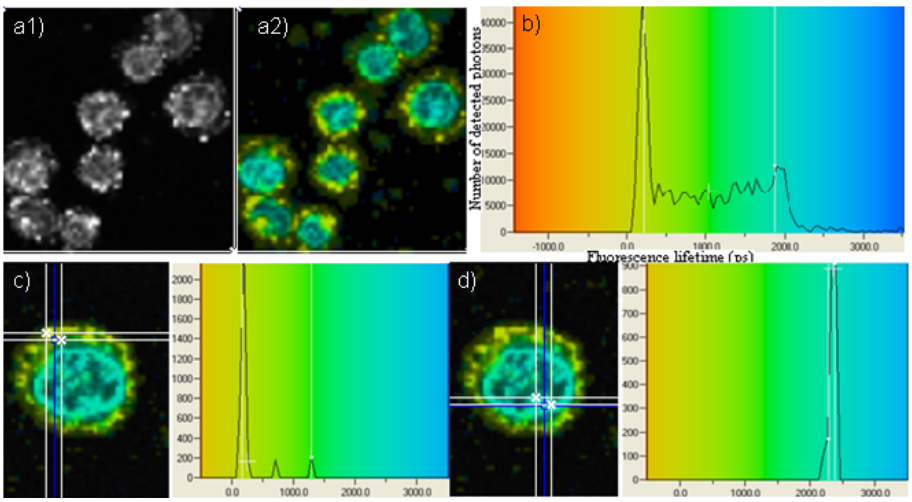

Fig.4. Multiphoton microscopy of Karpas 299 cells labeled with gold NPs and dyes H258. (a). Intensity image, corresponding false-color fluorescence lifetime image. (b). Histogram of lifetime distribution of photons within image frame (Excitation: 750nm, 16mw). (c) & (d). Deconvolution analysis for specific area of interest in image delivers the fluorescence lifetime of gold NPs and H258. (Zoom: 600).

4. CONCLUSION

In contrast with conventional one-photon imaging microscopy system, multiphoton excitation microscope provides attractive advantages and can be employed as novel noncontact biomedical tools for three-dimensional resolved fluorescence imaging, optical diagnostics, etc.[18-20] Because multiphoton excitation at high intensities occurs only in the minute focal volume of a high numerical aperture objective, photobleaching and photodamage are minimized in focus region[21]. FLIM offers powerful tools for investigating cancer detection with high time-resolution, high lifetime accuracy. Becker & Hickl system gives enough detail about the decay curve to enable multiexponent fitting. Several decay components in multi-exponential decay functions can clearly be distinguished. Accordingly, with the development of practical time-gated detection schemes, multiphoton FLIM could be used for clinical applications.

These preliminary experiments show clearly high resolution, sensitive intensity and lifetime images by investigating multiphoton imaging of cancer cells incubated with different optical probes. On the basis of different fluorescence lifetime distribution with these three optical probes, we can easily discriminate the imaging effect in different experiment conditions. Due to the specific conjugation of ACT1 and CD25, Au-ACT1 conjugates, and A488-ACT1 conjugates bind homogeneously and specifically to the surface of cell membrane of Karpas 299 (Figure 3(b)). In the same condition with 750nm, 20mw laser excitation, the emission intensity of gold NPs is stronger than that of cells. For the comparison of optical properties between gold NPs and fluorescent dye, we designed two different experimental conditions. High emission efficiencies of optical probes are observed comparing with biological cells. Through calculating the number of emission photons that is collected from the same eight pixels (Figure 4(c) and (d)), the emission photons of gold NPs is much more than that of H258. We also studied the phenomenon of photobleaching on a time scale for many minutes, and found that gold NPs has more photostable than the other fluorescent dyes.

The other important finding is the photo-thermolysis of gold NPs in laser irradiated target cells caused microbubbles around them and the cell destruction, but the same laser power were safe for cells. Some

studies have presented the photothermal destruction of gold NPs for killing cancer cells selectively[22-24]. The mechanism of nanoparticle-based techniques for cell necrosis is still unclear, though some papers have reported the possible mechanism [25, 26].

In summary, this study demonstrates that cellular imaging with improved contrast based on gold NPs and other fluorescent dyes, which is obtained using a NIR multiphoton excitation laser scanning microscope. Gold NPs are easily bioconjugated, and their special optical properties are unique in comparison with other optical probes. In future experiments we propose to choose different proper antibody to conjugate with gold NPs for imaging with different kinds of cells, and to study the efficiency of photo-thermolysis of gold NPs on normal cells and disease cells.

ACKNOWLEDGMENTS

We thank Research center Borstel supporting Karpas 299 cell lines, and thank their help during the preparation of immunooptical probes and samples. We acknowledge Barbara Flucke, Margit Kernbach, Bever Marco, and Astrid Rodewald at Institute of Biomedical Optics, Cuiping Yao at School of Life Science and Technology for their help during this experiment. This study was supported by the National Nature Science Foundation of China (Grant No. 60578026) and Project Based Personnel Exchange Programme with CSC and DAAD (2006).

REFERENCES

1. S. Weiss, “Fluorescence spectroscopy of single biomolecules,” Science **283** (5408), 1676-1683 (1999).
2. P. Alivisatos, “The use of nanocrystals in biological detection,” Nat. Biotechnol. **22** (1), 47-52 (2004).
3. X. Y. Wu, H. J. Liu, J. Q. Liu, K. N. Haley, J. A. Treadway, J. P. Larson, N. F. Ge, F. Peale, and M. P. Bruchez, “Immunofluorescent labeling of cancer marker Her2 and other cellular targets with semiconductor quantum dots", Nat. Biotechnol. **21**(1), 41-46 (2003).
4. X. Michalet, F. F. Pinaud, L. A. Bentolila, J. M. Tsay, S. Doose, J. J. Li, G. Sundaresan, A. M. Wu, S. S. Gambhir, and S. Weiss, “Quantum dots for live cells, in vivo imaging, and diagnostics,” Science **307** (5709), 538-544 (2005).
5. J. L. West and N. J. Halas, “Applications of nanotechnology to biotechnology - Commentary,” Curr. Opin. Biotech. **11** (2), 215-217 (2000).
6. J. Yguerabide and E. E. Yguerabide, “Light-scattering submicroscopic particles as highly fluorescent analogs and their use as tracer labels in clinical and biological applications - I. Theory,” Anal. Biochem. **262** (2), 137-156 (1998).
7. A. Shamsaie, M. Jonczyk, J. Sturgis, J. P. Robinson, and J. Irudayaraj, “Intracellularly grown gold nanoparticles as potential surface-enhanced Raman scattering probes,” J. Biomed. Opt. **12** (2), Art. No. 020502 (2007).
8. P. J. Campagnola, H. A. Clark, W. A. Mohler, A. Lewis, and L. M. Loew, “Second-harmonic imaging microscopy of living cells,” J. Biomed. Opt. **6** (3), 277-286 (2001).
9. S. Maiti, J. B. Shear, R. M. Williams, W. R. Zipfel, and W. W. Webb, “Measuring serotonin distribution in live cells with three-photon excitation,” Science **275** (5299), 530-532 (1997).
10. I. H. El-Sayed, X. H. Huang, and M. A. El-Sayed, “Surface plasmon resonance scattering and absorption of anti- EGFR antibody conjugated gold nanoparticles in cancer diagnostics: Applications in oral cancer,” Nano. Lett. **5** (5), 829-834 (2005).
11. P. T. C. So, C. Y. Dong, B. R. Masters, and K. M. Berland, “Two-photon excitation fluorescence microscopy,”

Annu. Rev. Biomed. Eng. **2**, 399-429 (2000).

12. B.A. Becker W, König K, Tirlapur U, "Picosecond fluorescence lifetime microscopy by TCSP imaging," Proc. SPIE Bios, 1-6 (2001).
13. K. Palo, L. Brand, C. Eggeling, S. Jager, P. Kask, and K. Gall, "Fluorescence intensity and lifetime distribution analysis: Toward higher accuracy in fluorescence fluctuation spectroscopy," Biophys. J. **83** (2), 605-618 (2002).
14. K. Sokolov, J. Aaron, B. Hsu, D. Nida, A. Gillenwater, M. Follen, C. MacAulay, K. Adler-Storthz, B. Korgel, M. Descour, R. Pasqualini, W. Arap, W. Lam, and R. Richards-Kortum, "Optical systems for In vivo molecular imaging of cancer," Technol. Cancer Res. T. **2** (6), 491-504 (2003).
15. R. A. Farrer, F. L. Butterfield, V. W. Chen, and J. T. Fourkas, "Highly efficient multiphoton-absorption-induced luminescence from gold nanoparticles," Nano. Lett. **5** (6), 1139-1142 (2005).
16. N. Panchuk-Voloshina, R. P. Haugland, J. Bishop-Stewart, M. K. Bhalgat, P. J. Millard, F. Mao, W. Y. Leung, and R. P. Haugland, "Alexa dyes, a series of new fluorescent dyes that yield exceptionally bright, photostable conjugates," J. Histochem. Cytochem. **47** (9), 1179-1188 (1999).
17. B. L. Sailer, A. J. Nastasi, J. G. Valdez, J. A. Steinkamp, and H. A. Crissman, "Differential effects of deuterium oxide on the fluorescence lifetimes and intensities of dyes with different modes of binding to DNA," J. Histochem.Cytochem. **45** (2), 165-175 (1997).
18. T. Gura, "Multiphoton imaging - Biologists get up close and personal with live cells," Science **276** (5321), 1988-1990 (1997).
19. S. Kantelhardt, J. Leppert, N. Petkus, G. Huttmann, V. Rohde, and A. Giese, "Multiphoton microscopy and fluorescence lifetime imaging of brain and brain tumor tissue," J. Neuro-Oncol. **8** (4), 494-494 (2006).
20. J. Leppert, J. Krajewski, S. R. Kantelhardt, S. Schlaffer, N. Petkus, E. Reusche, G. Huttmann, and A. Giese, "Multiphoton excitation of autofluorescence for microscopy of glioma tissue," Neurosurgery **58** (4), 759-767 (2006).
21. K. König, "Multiphoton microscopy in life sciences," J. Microsc-Oxford. **200**, 83-104 (2000).
22. J. Y. Chen, D. L. Wang, J. F. Xi, L. Au, A. Siekkinen, A. Warsen, Z. Y. Li, H. Zhang, Y. N. Xia, and X. D. Li, "Immuno gold nanocages with tailored optical properties for targeted photothermal destruction of cancer cells," Nano. Lett. **7** (5), 1318-1322 (2007).
23. C. P. Yao, R. Rahmanzadeh, E. Endl, Z. X. Zhang, J. Gerdes, and G. Huttmann, "Elevation of plasma membrane permeability by laser irradiation of selectively bound nanoparticles," J. Biomed. Opt. **10** (6) (2005).
24. I. H. El-Sayed, X. H. Huang, and M. A. El-Sayed, "Selective laser photo-thermal therapy of epithelial carcinoma using anti-EGFR antibody conjugated gold nanoparticles," Cancer Lett. **239** (1), 129-135 (2006).
25. C. M. Pitsillides, E. K. Joe, X. B. Wei, R. R. Anderson, and C. P. Lin, "Selective cell targeting with light-absorbing microparticles and nanoparticles," Biophy. J. **84** (6), 4023-4032 (2003).
26. G. Huttmann and R. Birngruber, "On the possibility of high-precision photothermal microeffects and the measurement of fast thermal denaturation of proteins," IEEE J. Sel. Top. Quant. Elect. **5**(4), 954-962 (1999).